GENERALIZED QUANTUM RESONANT CONVERTERS USING A NEW CONCEPTS OF QUANTUM RESONANT SWITCH

Gyu B. Joung, Jung G. Cho and Gyu H. Cho

Dept. of Electrical and Electronics Eng., Korea Advanced Institute of Science and Technology
P.O. Box 150, Chongnyansg, Seoul 130-650, Korea

ABSTRACT

For generalization of the soft switching based quantum resonant converters including ac/ac conversion applications, a new concept of quantum resonant switches which include quantum series resonant switch(QSRS) and quantum parallel resonant switch(QPRS), are proposed. The quantum resonant switches are modeled as equivalent inductor or capacitor, equivalent inductor for QSRS and equivalent capacitor for QPRS. The basic conventional PWM dc/dc and ac/ac converters can be changed to the corresponding quantum resonant converters with the same global characteristics by replacing the link inductor or capacitor with proposed QSRS or QPRS. Thus, the conventional modeling and design methods can also be applied for quantum resonant converters. In this procedure, a number of useful quantum resonant ac/ac converters which can improve the characteristics of the high frequency dc-link ac/ac converters, are newly suggested. The experimental verifications of modeling of the quantum resonant switches and the topologies and basic operations of newly proposed quantum resonant dc/dc and ac/ac converters are presented.

I. INTRODUCTION

In the switching power converters, the resonant conversion techniques have been renewed fast because of their well known merits such as high power density, high efficiency and high performance, etc. In consequence, a number of useful resonant dc/dc converters and high frequency dc-link ac/ac converters have been suggested to replace the conventional hard switched PWM converters[1-7]. However, many of them show different characteristics compared to those of the conventional PWM converters. Further, the high performance controller design is not easy task, since the modeling method of them are generally not known. To overcome these problem, the full bridge type quantum resonant dc/dc converters which have the same global characteristics as those of the conventional PWM converters and can easily be modeled, have been suggested[3-5] and thus, the conventional design and control methods can also be applied for these converters. In the case of high frequency dc-link, however, the modeling methods have not been known and the bulky dc-link inductor or capacitor are still required.

In this paper, the quantum resonant switches are proposed to generalize the quantum resonant converters. As a result of generalization, several useful topologies of quantum resonant ac/ac converters are suggested. The quantum resonant switches which consist of LC resonant circuit and several switches, are analyzed and modeled as equivalent inductor or capacitor, equivalent inductor for QSRS and equivalent capacitor for QPRS. Using these concepts, the inductor or capacitor in the conventional hard switching based PWM dc/dc converters can be replaced by QSRS or QPRS. Then, the zero current or zero voltage switching based quantum resonant dc/dc converters are obtained with the same global characteristics as those of the conventional PWM dc/dc converters. Similarly, the conventional dc-link PWM ac/ac converters can be changed to the corresponding quantum resonant ac/ac converters by replacing the dc-link inductor or capacitor with QSRS or QPRS. The quantum resonant ac/ac converters which are a kind of high frequency resonant dc-link ac/ac converters, have several advantages over the high frequency dc-link ac/ac converters such as small size of reactive elements by rejecting the dc-link inductor or capacitor, easy to model and control since they have the same global characteristics as those of the conventional hard switched PWM dc-link ac/ac converters and small VAR ratings of devices and reactive elements. Thus, the proposed quantum resonant ac/ac converters can be thought to be useful for high performance ac/ac conversion application.

Analysis and operations of QSRS and QPRS are described and modeling of them are derived analytically and verified by experiment. The basic topologies and operations of quantum resonant dc/dc and ac/ac converters are presented through the generalization of quantum resonant converters and the usefulness of the newly proposed quantum resonant converters.

II. QUANTUM RESONANT SWITCHES AND MODELS

A. Quantum Series Resonant Switches(QSRS's)

The quantum series resonant switches(QSRS's) and their models are shown in Fig. 1. The QSRS's which consist of LC series resonant circuit and several switches, are controlled by

CH2873-8/90/0000-0847 $1.00 © 1990 IEEE

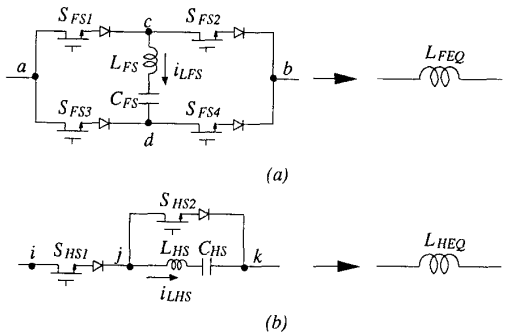

Fig. 1 Quantum series resonant switches(QSRS's) and their models: (a) full wave type, (b) half wave type.

integral cycle mode[4-6]. Thus, the current of switch module can be full and half wave rectified one of the resonant current according to the configuration of switches. The circuit topologies of full and half wave QSRS are shown in Fig. 1(a) and (b), respectively and their operations and modeling are described as follows.

(1) Full Wave QSRS

To perform the full bridge rectification of the resonant current, the S_{FS1} , S_{FS2} and S_{FS3} , S_{FS4} pairs are turned on and off alternately in synchronization with current zero crossing points. The waveforms of full wave QSRS are shown if Fig. 2. Since the voltage applied to LC resonant circuit, is in phase with the resonant current as shown in Fig. 2(b), the LC resonant tank is energized and thus th peak resonant current is increased as shown in Fig. 2(c). Fig. 2(d) shows the switch module current which is full bridge rectified one of the resonant current. Detailed analysis and modeling of the full wave QSRS are descrived as follows.

During the half resonant period, the resonant current $i_{LFS}(t)$ is half sinusoidal as shown in Fig. 2(c). The switch module current i_{FS} becomes

$$i_{FS} = i_{ab}(t) = | i_{LFS}(t) | . \tag{1}$$

During k-th resonant period, we can write

$$| i_{FS}(k) | = | i_{LFS}(k) | = \left(\frac{2}{\pi}\right) | i_p(k) | . \tag{2}$$

where $i_{FS}(k)$ is average value and $i_p(k)$ is peak value of the resonant current for the k-th resonant interval. From Fig. 1(a) and Fig. 2, we obtain

$$| i_{LFS}(t) | = \frac{\{v_c^*(k) + E_F\}}{Z} \sin\{\omega_r(t - kT/2)\}$$

$$kT/2 \le t < (k+1)T/2 \tag{3}$$

where $v_c^*(k)$ is absolute value of resonant capacitor voltage at the k-th switching instant, $\omega_r = 1/\sqrt{LC}$ and $T = 2\pi\sqrt{LC}$. Thus, the switch average current i_{FSA} for the k-th resonant period becomes

$$i_{FSA}(k) = i_{ab}|_{av} = \frac{2}{\pi}\frac{v_c^*(k) + E_F}{Z} . \tag{4}$$

From eq. (3), $v_c^*(k+1)$ becomes

$$v_c^*(k+1) = \frac{1}{CZ}\int_{kT/2}^{(k+1)T/2} \{v_c^*(k) + E_F\} \sin\{\omega_r(t - kT/2)\} - v_c^*(k) dt$$

$$= v_c^*(k) + 2E_F . \tag{5}$$

From eq. (4) and (5), we obtain

$$i_{FSA}(t) = i_{FSA}(k) \tag{6}$$

$$\frac{di_{FSA}(t)}{dt} = \frac{i_{FSA}(k+1) - i_{FSA}(k)}{T/2} \tag{7}$$

we obtain equivalent equation for the full wave QSRS module as follows :

$$\left(\frac{\pi}{2}\right)^2 L_F \frac{di_{SFA}(t)}{dt} = E_F . \tag{8}$$

From Eq. (8), we see that QSRS can be modeled as equivalent D.C. inductor and the equivalent inductance can be represented as follows.

$$L_{FEQ} = \left(\frac{\pi}{2}\right)^2 L_{FS} \tag{9}$$

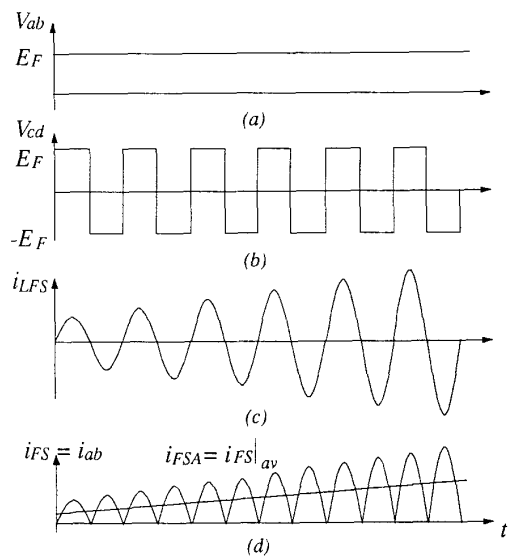

Fig. 2 Waveforms of the full wave QSRS: (a) voltage applied the to switch module, (b) voltage applied to the resonant circuit, (c) resonant current, (d) switch module current.

(2) Half wave QSRS

In the half wave QSRS module, S_{HS1} and S_{HS2} are turned on and off alternately in synchronizations with the current zero crossing points of the resonant current. Fig. 3 shows switching operation and waveforms of half wave QSRS shown in Fig. 1(b). The switch module current i_{HS} becomes resonant inductor current when S_{HS1} is turned on and it becomes zero when S_{HS2} is turned on. Therefore, the slop of average switch module current i_{HSA} is quarter value of the full wave QSRS module as shown in Fig. 3(d). Equivalent inductance of the half wave QSRS module is given by $4(\pi/2)^2 L_{HS}$. Analytical modeling procedure are similar to those of the full wave QSRS module. The resultant equivalent equation is as follows :

$$L_{HEQ}\frac{di_{HS}(t)}{dt} = E_H \tag{10}$$

where

$$L_{HEQ} = \pi^2 L_{HS}. \tag{11}$$

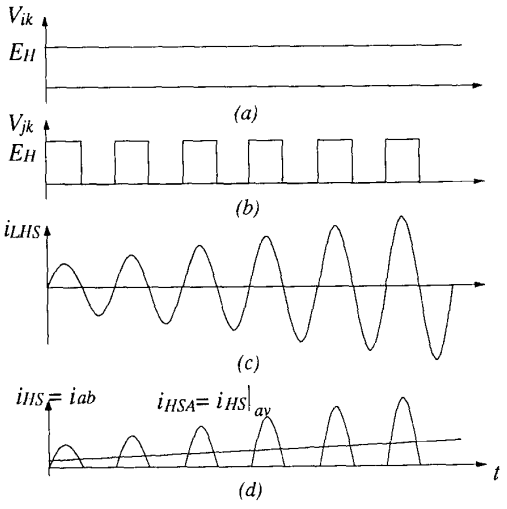

Fig. 3 Waveforms of the half wave QSRS: (a) voltage applied to the switch module, (b) voltage applied to the resonant circuit, (c) resonant current, (d) switch module current.

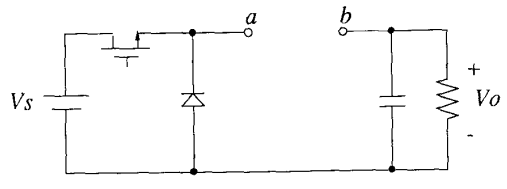

Fig. 4 Test circuit for QSRS's: QSRS's and their equivalent inductors are connected between the terminal a and b, in turn.

(3) Experimental Verifications of the QSRS's

To verify the modeling of the QSRS's, the simple test circuit is constructed as depicted in Fig. 4 and the full and half wave QSRS's and their models, equivalent inductors, are connected in turn between terminal a and b. Fig. 5(a) and (b), show the current waveforms of full wave QSRS and its equivalent inductor when the test circuit is controlled with duty ratio of 6/9. As can be seen from Fig. 5(a) and (b), the average current of the full wave QSRS is linearly varied and its slop is almost equal to that of the equivalent inductor current. Fig. 6(a) and (b), show the current waveforms of the half wave QSRS and its equivalent inductor when the duty ratio is 3/5. The slop of average current are also equal to the current of the equivalent inductor. we can see that, however, the value of equivalent inductance is four times of that of the full wave QSRS.

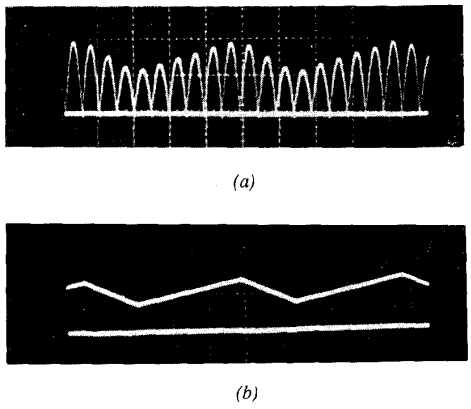

(a)

(b)

Fig. 5 Experimental waveforms of the full wave QSRS and its equivalent inductor: (a) QSRS current, (b) equivalent inductor current. Vert; 10A/Div., Time base; 10usec/Div.

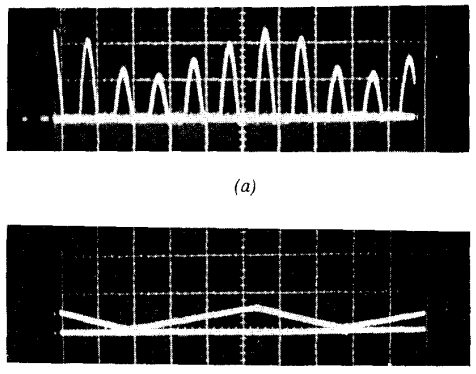

(a)

(b)

Fig. 6 Experimental waveforms of the half wave QSRS and its equivalent inductor: (a) QSRS current, (b) equivalent inductor current. Vert; 10A/Div., Time base; 10usec/Div.

B. Quantum Parallel Resonant Switches(QPRS's)

The quantum parallel resonant switches(QPRS's) and their models are shown in Fig. 7. The QPRS's consist of the LC parallel resonant circuit and several switches and are also controlled by integral cycle mode. All switches are also turned on and off in synchronization with the voltage zero crossing points so that the switch module voltages are full or half bridge rectified ones of resonant voltage. The switching operations and waveforms of the full and half wave QPRS's are dual with those of the QSRS module as shown in Fig. 8 and 9. By neglecting the high frequency ripple components, the average values of switch voltages v_{FP} and v_{HP} are linearly increased as shown in Fig. 8 and 9. The analytical modeling procedure of the QPRS's are also similar to those of QSRS. Resultant equations are as follows :

(1) Full wave QPRS

$$C_{FEQ}\frac{dv_{FPA}(t)}{dt}=I_F \tag{12}$$

where

$$C_{FEQ}=\frac{\pi^2}{2}C_{FP}. \tag{13}$$

(2) Half wave QPRS

$$C_{HEQ}\frac{dv_{HPA}(t)}{dt}=I_H \tag{14}$$

where

$$C_{HEQ}=(\pi)^2 C_{HP}. \tag{15}$$

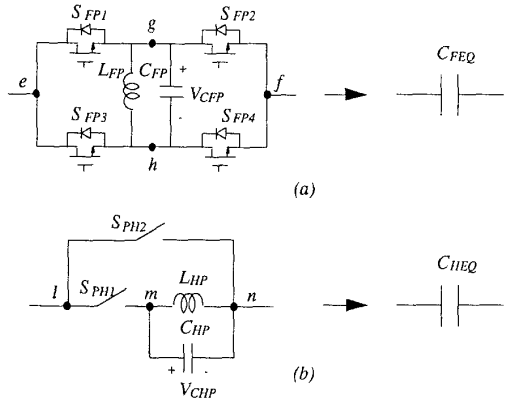

Fig. 7 Quantum parallel resonant switches(QPRS's) and their models: (a) full wave type, (b) half wave type.

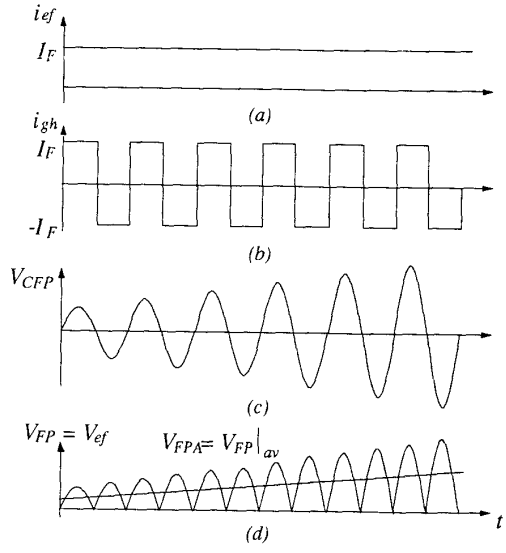

Fig. 8 Waveforms of the full wave QPRS: (a) voltage applied to the switch module, (b) voltage applied to the resonant circuit, (c) resonant current, (d) switch module current.

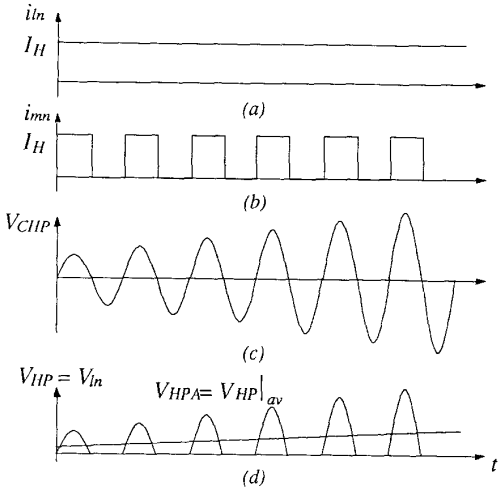

Fig. 9 Waveforms of the half wave QPRS: (a) voltage applied to the switch module, (b) voltage applied to the resonant circuit, (c) resonant current, (d) switch module current.

(3) Experimental Verifications of the QPRS's

The test circuit is also constructed to verify the modeling of QPRS as depicted in Fig. 10. Fig. 11 and 12 show the voltage waveforms of the full and half wave QPRS's and their equivalent capacitors with duty ratios of 4/8 and 2/4, respectively. As can seen from Fig. 11 and 12, the slops of the average voltage waveforms are well matched to those of their equivalent

capacitors, respectively. The value of the equivalent capacitance of the half wave QPRS is also four times of that of the full wave QPRS.

From these analytical and experimental verifications, the QSRS modules are modeled as dc inductor and the QPRS modules are modeled as dc capacitor. If the all switches are replaced with bidirectional ones, the QSRS and QPRS are modeled as AC inductor or capacitor, respectively.

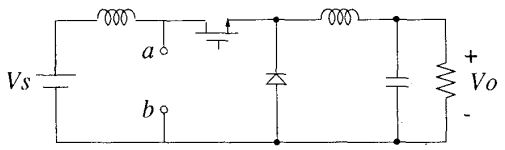

Fig. 10 Test circuit for the QPRS's: QPRS's and their equivalent capacitors are connected between the terminal a and b, in turn.

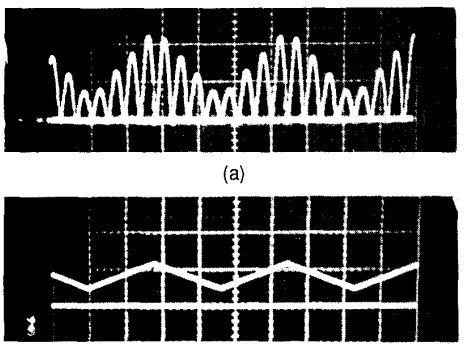

Fig. 11 Experimental waveforms of the full wave QPRS and its equivalent capacitor: (a) QPRS voltage, (b) equivalent capacitor voltage. Vert; 10V/Div., Time base; 10usec/Div.

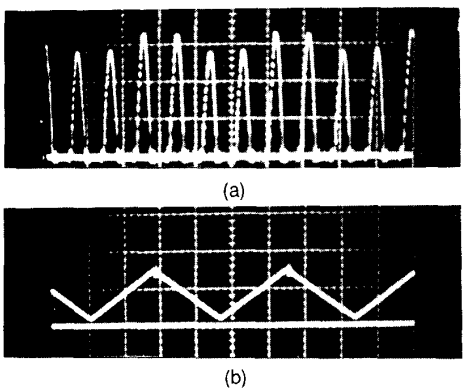

Fig. 12 Experimental waveforms of the half wave QPRS and its equivalent capacitor: (a) QPRS voltage, (b) equivalent capacitor voltage. Vert; 10V/Div., Time base; 10usec/Div.

III. GENERALIZED QUANTUM RESONANT CONVERTERS

A. Quantum Resonant dc/dc Converters

The 4-basic conventional PWM dc/dc converters can be changed to the corresponding quantum resonant converters by using the proposed QSRS or QPRS. The 4-basic quantum resonant dc/dc converters are obtained as shown in Fig. 13 by replacing the inductor or capacitor of the PWM converters with the half wave QSRS or QPRS which are chosen to reduce the number of switches. In this case, the switch S_{HS1} of half wave QSRS depicted in Fig. 1(b) is unnecessary, since it is overlapped with the main switch of converters.

To illustrate the basic operation of newly constructed quantum resonant dc/dc converters, the buck type quantum resonant converter is chosen and its operational mode diagrams and waveforms are shown in Fig. 14 and 15, respectively. As can be seen, the basic operation is very similar to that the buck type PWM dc/dc converter. The average inductor current is linearly increased or decreased according to powering or freewheeling modes and its slop is the same as that of the equivalent inductor which is caused by the modeling of the half wave QSRS. Thus, the conventional modeling and design techniques are also available for the quantum resonant dc/dc converters. The output voltage is controlled by the duty ratio of powering period to total switching period. The quantized phenomina, however, is occurred in duty ratio and output voltage since the switching instants are synchronized with the zero crossing points of the resonant current.

The operations of the other converters, are also very similar to those of the PWM converters and their models are also obtained easily by applying the models of quantum resonant switches.

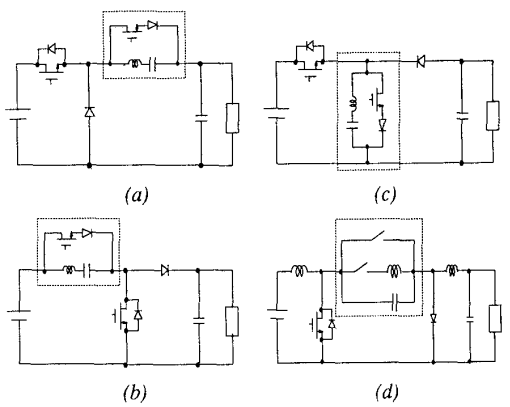

Fig. 13 New topologies of the quantum resonant dc/dc converters with the half wave QSRS or QPRS: (a) buck type, (b) boost type, (c) buck-boost type, (d) cuk type.

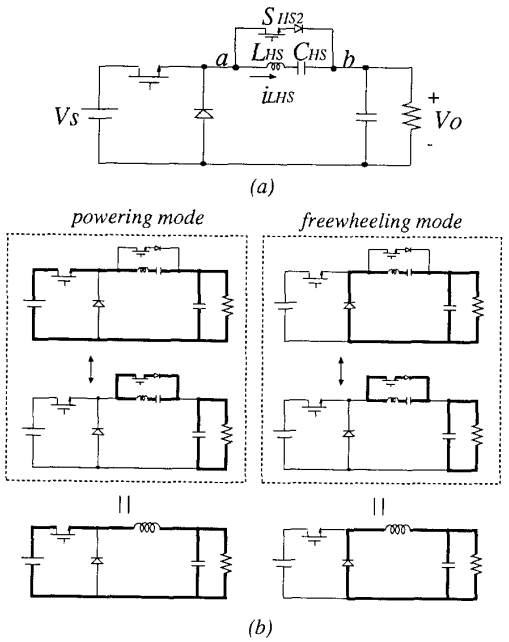

Fig. 14 Basic operational mode diagrams of the buck type quantum resonant converter and the PWM converter for comparison: (a) circuit topology, (b) comparison of the operational mode diagrams

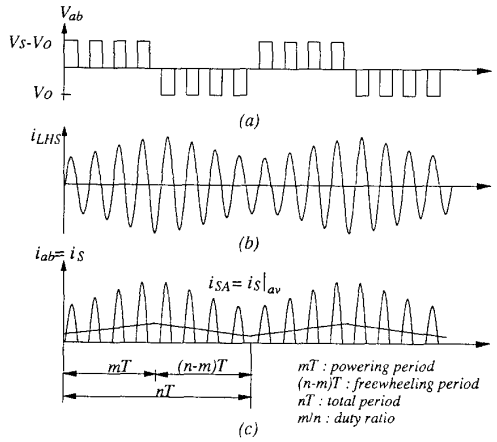

Fig. 15 Waveforms of the buck type quantum resonant converter: (a) voltage applied to the resonant circuit of QSRS, (b) resonant current, (c) switch module current.

B. Quantum Resonant ac/ac Converters

As the case of dc/dc converters, the conventional dc-link ac/ac converters can be changed to the corresponding quantum resonant ac/ac converters by replacing dc-link inductor or capacitor with the QSRS or QPRS, respectively. Consequently, several new topologies of the quantum resonant ac/ac converters which are a kind of high frequency dc-link ac/ac converters, are obtained as shown in Fig. 16 and 19. Fig. 16 shows the quantum series resonant ac/ac converters using the full and half wave QSRS's, which are obtained from the conventional dc-current-link ac/ac converter. The basic operations of the full and half wave quantum series resonant converters are shown in Fig. 17 and 18, respectively and compared to those of the PWM dc-link ac/ac converters to illustrate analogous global characteristics between them.

The switching patterns are provided so that the dc-link currents are full or half bridge rectified currents of each LC resonant currents and its average currents are controlled with powering, freewheeling and regenerating modes as the conventional PWM dc-link converters do. As can be seen form Fig. 17(b) and 18(b), the average link currents are well matched to those of the conventional PWM converters. Therefore, the modeling and design techniques of the PWM dc-link ac/ac converters can also be applied for the quantum resonant ac/ac converters.

Fig. 19 shows the quantum parallel resonant ac/ac converters using the full and half wave QPRS, which are obtained from the conventional dc-voltage-link ac/ac converter. The circuit topology of the full wave quantum parallel resonant ac/ac converter depicted in Fig. 19(a) has been presented as a resonant dc-link ac/ac converter[7]. However, the modeling and effective control laws have not been known yet. The operation of the quantum parallel resonant ac/ac converters can easily be explained by applying the duality between the QSRS and QPRS. So, the waveforms of resonant voltage and dc-link voltage would be similar to the current waveforms of the quantum series resonant ac/ac converters.

C. Usefulness of the Quantum Resonant Converters

The generalization of the quantum resonant converters is

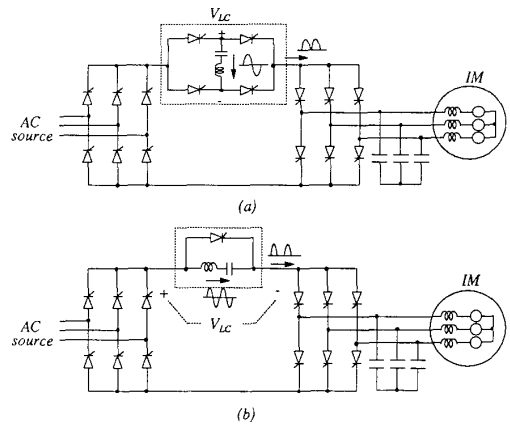

Fig. 16 Circuit topologies of the quantum series resonant ac/ac converters using (a) full wave QSRS, (b) half wave QSRS.

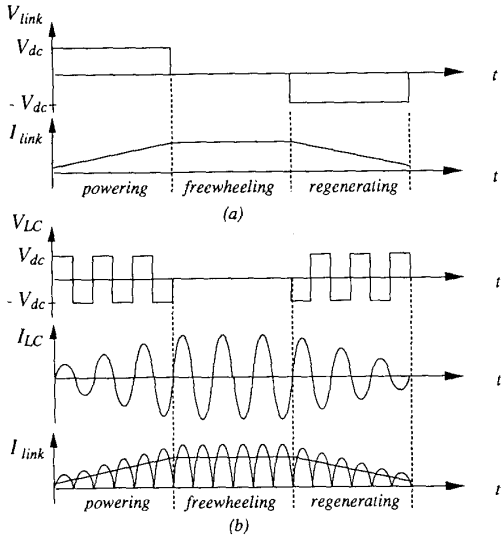

Fig. 17 Waveforms of the dc-link current and voltage applied tc the link: (a) conventional dc-link ac/ac converter with the equivalent dc-link inductor, (b) full wave mode quantum resonant ac/ac converter.

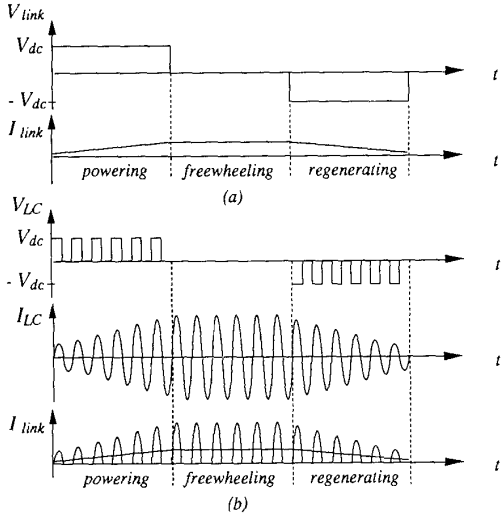

Fig. 18 Waveforms of the dc-link current and voltage applied tc link: (a) conventional dc-link ac/ac converter with the equivalent dc-link inductor, (b) half wave mode quantum resonant ac/ac converter.

performed by using the new concept of quantum resonant switches. In consequence, the new topologies of the quantum resonant dc/dc and ac/ac converters are suggested. The quantum resonant dc/dc converters, however, may not be useful because

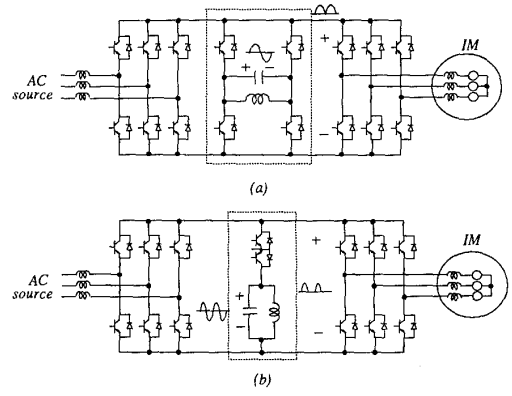

Fig. 19 Circuit topologies of the quantum parallel resonant ac/ac converters using (a) full wave QPRS, (b) half wave QPRS.

of increasing number of switches, large current ripple and quantized characteristic in output voltage.

On the other hand, the quantum resonant ac/ac converters have several distinctive advantages over the high frequency dc-link ac/ac converters such as small size of reactive elements by rejecting the dc-link inductor or capacitor, easy to model and control since they have the same global characteristics as those of the conventional PWM dc-link ac/ac converters. Though the number of the switches are more than that of the high frequency resonant dc-link ac/ac converter, it is not serious problem since the VAR ratings of the devices and reactive elements are very small and the semiconductor device cost is steadily decreasing.

IV. CONCLUSION

To generalize the quantum resonant converters, a new concept of quantum resonant switches is proposed and modeled as equivalent inductor or capacitor, equivalent inductor for QSRS and euivalent capacitor for QPRS. The modeling of the quantum resonant switches are confirmed through the experimental verifications. Using the quantum resonant switch concept, the topologies of the ZCS or ZVS based quantum resonant dc/dc and ac/ac converters which have the same global characteristics as those of the conventional PWM converters, are obtained and their operations are briefly described.

As a result of generalization, the quantum resonant ac/ac converters are newly suggested, which have distinctive advantages over the high frequency resonant dc-link ac/ac converters as follows:

(1) small size of the reactive elements,
(2) easy to model
(3) easy to design and control
(4) small VAR ratings of devices and reactive elements (in the full wave QSRS case)

Thus, the proposed quantum resonant ac/ac converters can be thought to be useful of high performance ac/ac conversion applications.

REFERENCE

[1] K. H. Liu, R. Oruganti and F. C. Lee, "Quasi-resonant converter -- topologies and characteristics, " IEEE Trans. on Power Electronics, vol. PE-I, No.1, PP. 62~71, Jan.1987

[2] D. M. Divan, " Diode as pseudo active elements in high frequency dc/dc converters" IEEE Trans. on Power Electronics, Vol. 4, No. 1, Jan. 1989.

[3] G. B. Joung, C. T. Rim, and G. H. Cho" An integral cycle mode control of series resonant converter," IEEE PESC Rec., PP. 575~582, 1988

[4] G. B. Joung, C. T. Rim and G. H. Cho," Modeling of quantum series resonant converter -- controlled by integral cycle mode," IEEE IAS Rec., PP. 821~826, 1988.

[5] G. B. Joung, and G. H. Cho," Modeling of quantum parallel resonant converters -- controlled by integral cycle mode," IEEE PESC Rec., PP. 82, PP. 744-751, 1989.

[6] Y. Murai and T. A. Lipo, "High frequency series resonant dc-link power conversion", IEEE IAS Rec., PP.308-313, 1988.

[7] D. M. Divan, "The resonant dc-link converter -- A new concept in static power conversion", IEEE IAS Rec., 648-656, 1986.